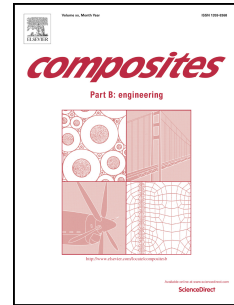# Journal Pre-proof

Evolution of the bearing failure map of pinned flax composite laminates aged in marine environment

V. Fiore, L. Calabrese, T. Scalici, A. Valenza

Please cite this article as: Fiore V, Calabrese L, Scalici T, Valenza A, Evolution of the bearing failure map of pinned flax composite laminates aged in marine environment, *Composites Part B* (2020), doi: https://doi.org/10.1016/j.compositesb.2020.107864.

This is a PDF file of an article that has undergone enhancements after acceptance, such as the addition of a cover page and metadata, and formatting for readability, but it is not yet the definitive version of record. This version will undergo additional copyediting, typesetting and review before it is published in its final form, but we are providing this version to give early visibility of the article. Please note that, during the production process, errors may be discovered which could affect the content, and all legal disclaimers that apply to the journal pertain.
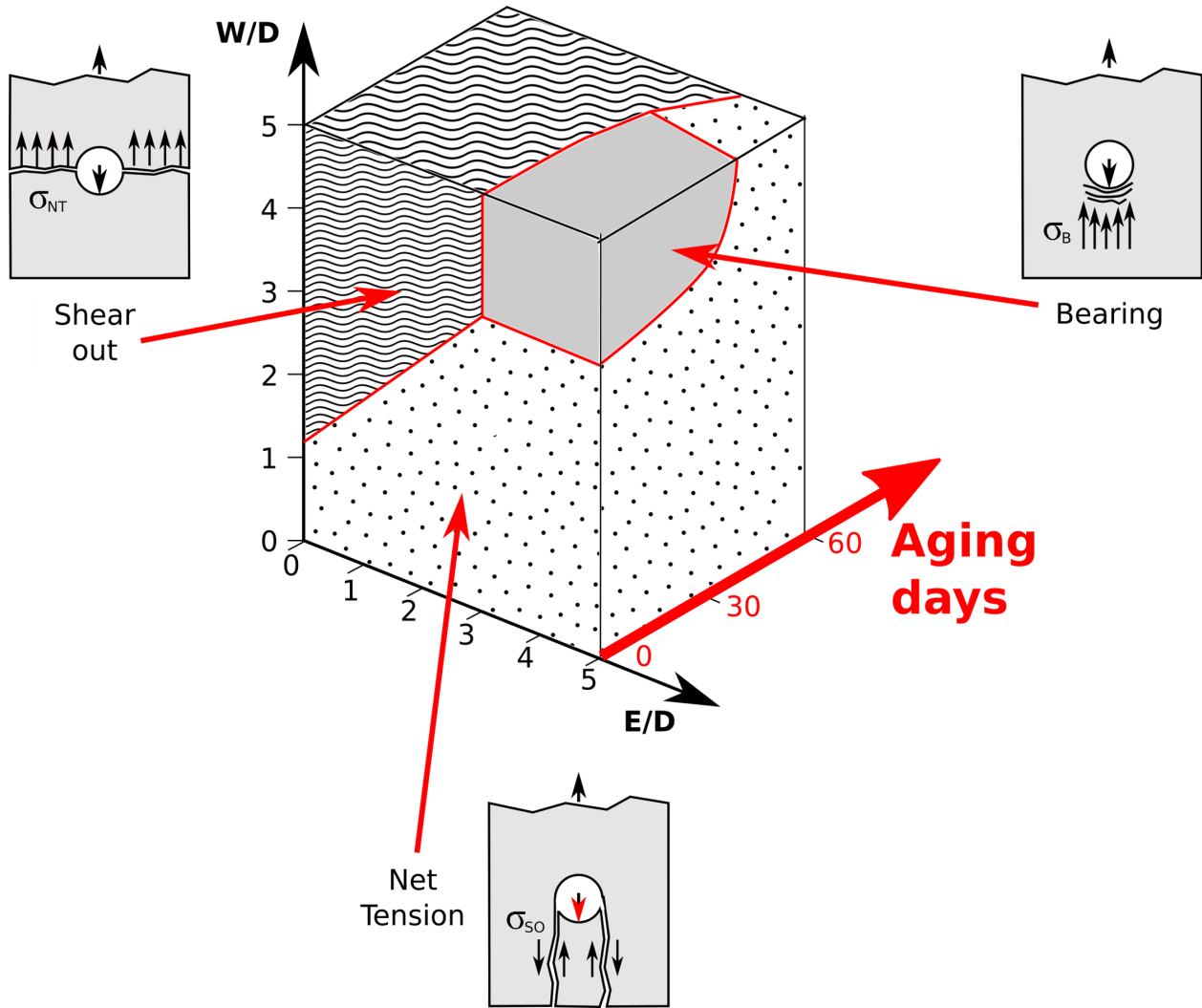
Evolution of the bearing failure map of pinned flax composite laminates aged in marine environment

V. Fiore[1*], L. Calabrese[2], T. Scalici[3], A. Valenza[1]

[1] Department of Engineering, University of Palermo

Viale delle Scienze, Edificio 6, 90128 Palermo, Italy

Email: vincenzo.fiore@unipa.it

[2] Department of Engineering, University of Messina

Contrada Di Dio (Sant'Agata), 98166 Messina, Italy

[3]School of Mechanical and Aerospace Engineering, Queen's University Belfast,

Ashby Building, Stranmillis Road, BT9 5AH Belfast

*Corresponding Author

Aim of the present paper is to evaluate how the bearing behavior of pinned flax composites can be influenced by their exposition to critical environment such as marine one. To this scope, flax fibers/epoxy pinned laminate was exposed up to 60 days to salt-fog environment, according to ASTM B 117 standard.

In particular, samples having different hole diameter (D), laminate width (W), and hole center to laminate free edge distance (E) have been tested under single lap bearing tests at varying the aging exposition time. Following this procedure, an experimental 2D failure map clustering main failure modes was created by placing the experimental results in the plane E/D versus W/D ratios, and its variation was analyzed at varying the aging exposition.

Experimental results showed that environmental aging induced modification on the mechanical performances of the pinned composite. Furthermore, the failure map, defined by E/D and W/D ratios axes, evidenced a progressive modification of damage mechanisms transitions, at increasing the exposition time. In particular, due to significant reductions of tensile and shear strengths of flax laminate, the progressive fracture by bearing mode was not observed for aged samples, replaced by premature and catastrophic shear out and net tension mechanisms.

1 Introduction

Fiber reinforced polymers (FRPs) have replaced, over the last decades, traditional materials in several engineering fields, such as nautical, aerospace, sports equipment. In particular, most of nautical structures are nowadays manufactured in FRPs due to their good compromise between low weight and high mechanical and chemo-physical properties. In this field, FRPs have been used since about the 1950s to partially replace traditional metallic materials like steel or aluminum alloys. The implementation of FRPs in conjunction with metals into hybrid structural systems is currently developed in nautical structures: i.e., the ship hulls are realized by using FRP materials due to their high stiffness whereas materials with high strength such as metal alloys are often used for the topside structures [1]. Hence, the combination of metallic materials together with FRPs have received growing attention both from the shipyard and from the academia [2–4] .

It is widely known that there are two kind of structural joining methods: i.e., mechanical and adhesive ones. Adhesive joints show advantages such as avoiding of delamination phenomena due to the absence of holes, reduction of the weight structure due to the absence of inserts and prevention of degradation phenomena caused by galvanic corrosion but the use of structural adhesives doesn't allow subsequent disassembly for maintenance and repair operations. As a consequence, mechanical joints (i.e., bolting, riveting, etc.) often represent the most suitable choice also taking into account their capability to sustain higher loads as well as their easy of assembly. In order to optimize the use of mechanical connections in composite or hybrid structures, the exploitation of the bearing behavior of pinned composite laminates has been investigated in previous papers concerning polymeric composites reinforced mainly with synthetic fibers such as glass [5–11] and carbon [12–15]. Furthermore, the influence of the geometrical configuration of pin-loaded composites on their bearing performances and failure modes

was recently investigated also for flax and glass-flax reinforced hybrid structures in our recent papers [16,17].

In particular, the bearing stress evolution and failure modes (i.e., bearing, net tension, shear out and cleavage) were investigated at varying pin diameter (D) and distance between the center hole and the sample free edge (E). Then, an experimental failure map, identifying the above failure modes, was obtained as function of the investigated geometrical parameters (E, D) and a theoretical model was overlapped with the experimental results. Following this procedure, the minimum values of E/D and W/D ratios to be chosen to avoid catastrophic failures (i.e., net tension, shear out or cleavage) were identified for each investigated stacking sequences. In particular, it was found that these limit values must be higher in the case of full flax reinforced laminates [16] in comparison to full glass ones [6], mainly due to the different mechanical properties of these laminates. On the other hand, glass-flax hybrid structures evidenced an intermediate behavior [17].

Despite the wide available literature about the bearing behavior of FRPs materials [7] [18] [19] [5] to the best of our knowledge no attempts were done until now on the evaluation of the effect of critical environments exposition on the mechanical behavior of pinned composites. In particular, due to the widespread use of composites structures as nautical components, the knowledge of how the bearing behavior of pinned FRP laminates can be influenced by the exposition to the marine environment is of upmost importance for the designers, especially when natural fibers are used as reinforcement.

For these reasons, the same flax-epoxy laminate investigated in an our previous paper [16] was aged under salt-fog spray conditions up to 60 days in order to evaluate the induced modification on the mechanical performances of the pinned composite joint. Furthermore, the evaluation of the experimental and theoretical failure maps at varying

joint geometry was also investigated, thus also evidencing how the critical values of E/D and W/D ratios can be altered in marine environment.

2   Material and methods

A panel with area 350 x 350 mm^2 was manufactured by means of vacuum assisted resin infusion technique and cured at 25 °C for 24 hours and post-cured at 50 °C for 8 hours. A DEGBA epoxy resin (commercial name SX8 EVO) supplied by Mates Italiana (Italy) and ten laminae of 2x2 twill weave woven flax fabric (318 g/m^2 areal weight) supplied by Lineo (France) were used as matrix and reinforcement, respectively. Bearing mechanical tests were carried out on prismatic samples with length 150 mm, according to ASTM D5961/D standard (procedure A), using a universal testing machine Z250 (Zwick-Roell, Germany), equipped with a 250 kN load cell, setting the displacement rate equal to 0.5 mm/min. The average fiber and void contents of the laminate and its nominal thickness are reported in our previous paper [16]. The samples geometry and the bearing test set-up are shown in Figure 1. Prismatic samples were cut by using a band saw and drilled by using at first an undersized drilling bits and then a mill tool to obtain the hole diameter without edge defects.
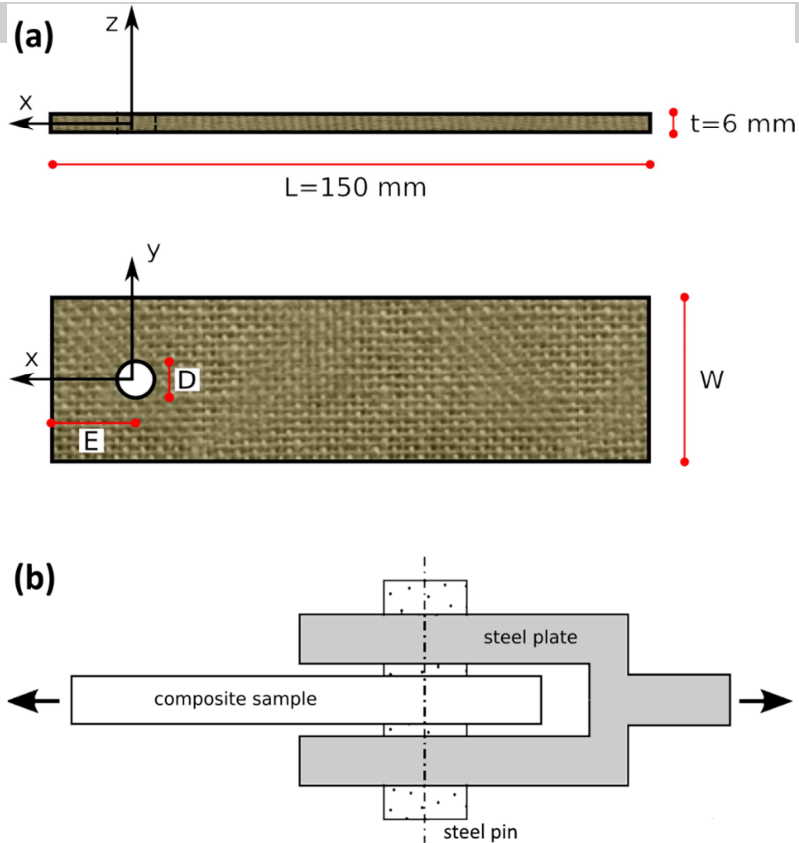
Figure 1. (a) Geometry of bearing specimens and (b) schematization of bearing test set-up

Aging exposition was carried out by using an Angelantoni (Italy) DCTC 600 climatic chamber, following the ASTM B 117 standard. The salt fog had a chemical composition of 5% NaCl solution (pH between 6.5 and 7.2) and the temperature was set equal to 35 °C. Single specimens were taken out from the climatic chamber after 30 and 60 days and mechanically tested with the aim to study the influence of salt-fog exposition on the bearing behaviour of each investigated laminate.

The obtained samples are codified as "FA", "FB" and "FC" depending if the flax laminate was aged 0, 30 or 60 aging days, respectively. The previous code was coupled with a lot of number xx-xx-xx that indicates the hole diameter (D), the edge distance (E) and sample width (W), respectively. E.g. FB-4-16-15 designates the flax laminate aged 30 days, with hole diameter, edge distance and sample width equal to 4 mm, 16 mm and 15 mm, respectively.

6

performed by using the bearing stress determined according to the following equation:

$$\sigma = P/(D * s)$$ **Eq. 1**

Where P is the applied load, D and s are the hole diameter and sample thickness respectively. The product D*s is indicated as bearing area where roughly fastener interacts with composite laminate. In the following paragraphs the joints stress was evaluated by using Eq. 1, regardless of the failure mechanism experimentally occurred.

3 Results and discussion

3.1 Stress-displacement curve analysis

3.1.1 Pinned joints with 4 mm hole diameter

Figure 2 shows the bearing stress versus displacement curves for flax laminates characterized by diameter, D = 4 mm, width W = 15 mm and edge distance E=16 mm (i.e. W/D = 3.75 and E/D = 4.0). After a short stabilization phase, due to tools adjustments, all curves initially show a linear relationship between stress and displacement. At increasing displacement, a gradual deviation from the linear trend can be observed. This behavior is due to compression collapse of the matrix in correspondence of the composite laminate just behind the small hole/pin contact area. All specimens tend to reach a plateau region at which a maximum stress is found, beyond which the specimen fails.

At varying aging time, a change in the stress-displacement trend can be highlighted. The unaged flax laminate shows good mechanical stability: i.e., it evidences a slight loss of linearity above about 120 MPa stress after which a progressive increase in stress at increasing displacement is observed up to reach a maximum stress at about 200 MPa. All the specimens showed a bearing failure mechanism.

performances induced by the exposition to the salt-fog. A significant reduction of the maximum stress takes place: i.e., about 25% and 35% lower than unaged sample (i.e., batch A) for batches B and C, respectively. Moreover, the displacement becomes more significant at low stress levels as can be seen by the wide plateau region detected in the 3.0-4.5 mm displacement range. Under salt-fog environment, flax fiber composites undergo a gradual absorption of water which leads to the triggering of softening phenomena of the matrix that are responsible for the reduction of mechanical performances even for short aging times [20]. In addition, water molecules can have physical and chemical effects on the inherently hydrophilic fibers and on fiber/matrix interface. Consequently, the adhesion loss implies a reduction of both strength and stiffness due to the limited transfer of stresses.
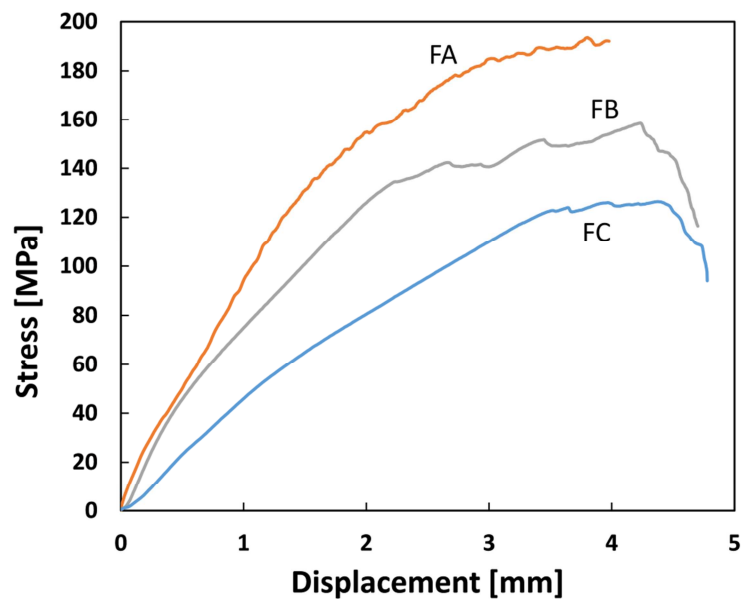

Figure 2. Stress-displacement curves at increasing aging time for pin loaded laminates (D = 4 mm; E = 16 mm; W = 15 mm)

This significant modification of the mechanical behavior of the flax laminate also involves a change of the occurring failure mechanism. In particular, at increasing the exposition time to the aggressive environment, a transition from bearing to net tension

of aging.

Further interesting information can be extrapolated by analyzing the fracture images of the samples at varying aging time (Figure 3).
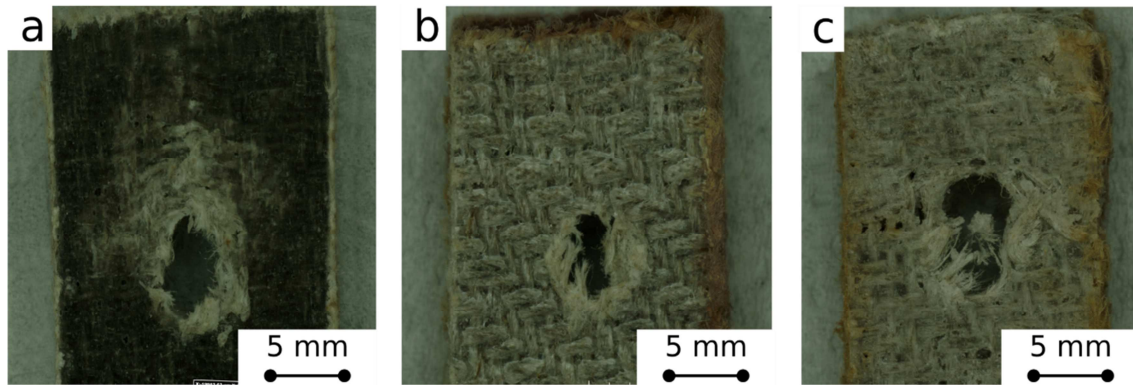

Figure 3. Fracture images of a) FA-4-16-15 b) FB-4-16-15 and c) FC-4-16-15 samples

The fracture image of FA-4-16-15 unaged sample (Figure 3a) highlights a compression collapse area on the pin/hole contact surface area due to bearing failure mechanism occurred. Furthermore, kink bands evolving radially from hole edge can be also identified, thus indicating a progressively extension of the damaged zone, referred as failure process zone. This phenomenon favors the collapse of the laminate due to the triggering of synergistic damage mechanisms such as delamination [19]. In fact, kink bands, which develop at compression due to plastic micro-buckling, induce strong local deformations at the fiber-matrix interface that, as a consequence, activate secondary failure premature modes [21]. Therefore, a damage accumulation process is triggered coupling fiber plies kink bands, shear cracks and delamination at the layers interface that evolve to a large-scale delamination phenomenon, thus leading to a decrease in the mechanical joint stability [16].

This phenomenon cannot be observed on 30 days aged samples (Figure 3b). The failure, although still associated with a compression bearing fracture, does not highlight large kink bands toward the free edges of the sample. On the contrary, only a local collapsed

be ascribed to the matrix softening due to the humid environment exposition. Analogously, Malmstein et al. [22] evidenced that the failure mode of composites severely affected by water becomes less brittle after hygrothermal aging, thus reducing cracking phenomena and stimulating a fiber/interface dominated fracture.

On the other hand, a different failure mechanism can be evidenced on FC-4-16-15 sample (Figure 3c), due to the long exposition time to the salt-fog environment: i.e., the specimen does not show a bearing collapse zone whereas a net tension fracture takes place, thus stimulating the activation and propagation of cracks orthogonally to the load direction, at the maximum stress concentration section. It can be evidenced the appearance of fiber breaking, mainly ascribed to the lowering of the flax tensile strength due to the long exposition (i.e., 60 days) to salt-fog environment.

Additional information can be acquired by evaluating the maximum bearing stress variation at increasing edge distance (Figure 4), keeping constant D and W (i.e., equal to 4 mm and 15 mm, respectively). The experimental trend highlights that the maximum bearing stress (σ_b) increases by increasing E/D ratio until a critical threshold value has been reached, as shown previously [23] [24].
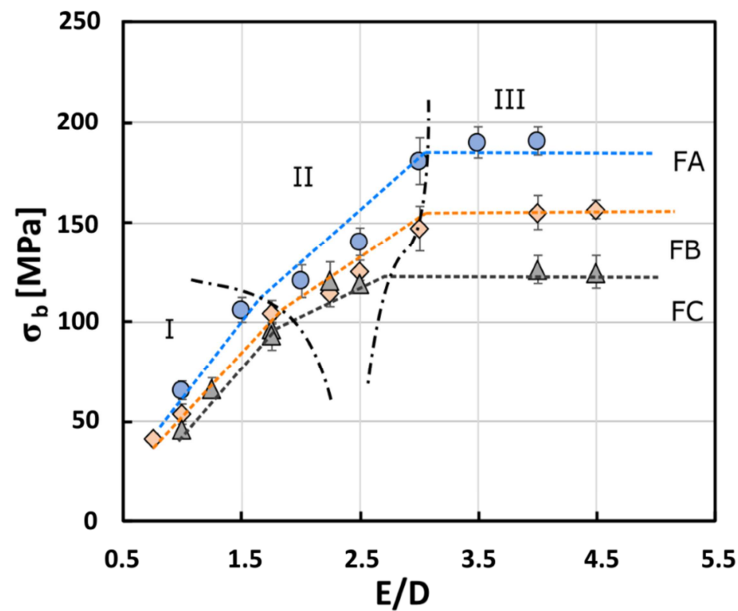
Figure 4. Maximum bearing stress evolution at increasing edge distance E for pin loaded laminates with hole diameter D = 4 mm and width W = 15 mm (W/D = 3.75) for all batches

For all composite batches, three linear segments have been identified associated with three distinct fracture mechanisms. In particular, a small distance of the hole from the edge favors the initiation and propagation of the fracture by shear out mode (region I). The region just behind the pin, that suffers the applied stress, is very limited (distance E is between 4 mm and 6 mm), therefore a catastrophic fracture (i.e., shear out) at very low stress values has been observed. However, as confirmed by the high slope of first fitting linear segment, the stress is very sensitive to edge distance: i.e., a slight increase in E implies a significant increase in the maximum stress. Subsequently, for medium values of E distance, with E/D in the range about 1.5-3.0, the failure mechanism for cleavage was observed (region II). This region progressive is reduced in extension at increasing aging time. As already discussed, the cleavage can be considered as a failure mechanism induced by the combination of shear out and net tension modes [5] and it usually is triggered from the joint edge rather than near to the hole area [8]. The cleavage is a type of catastrophic and immediate fracture mode, which leads to a

11

the mechanical strength of the joint is still influenced by the distance from the edge (E). However, a slope variation is evident with respect to what has been found for the shear breaking region.

For edge distance higher than 12 mm (i.e., E/D > 3), the maximum stress becomes constant (region III). In this region, the pin-loaded laminates undergo a mixed fracture mode between net tension and bearing mechanisms, thus suggesting that this specific pinned joint geometry implies a competition between such failure mechanisms. For unaged laminates, the prevailing mechanism is in any case bearing [16]. However, for 1 month aged specimens (i.e., batch B), there is an increase in net tension contribution in the fracture of the joint whereas just net tension fracture mechanisms were observed for the 2 month aged specimens (i.e., batch C).

The water aging degrades significantly the mechanical performances of the flax fibers, inducing a reduction both of their maximum stress and elastic modulus up to 40% [25]. It is well known that microstructure of flax fibers can be considered as a laminate with layers reinforced by cellulose micro-fibrils that are grouped in bundles to form meso-fibrils [26] [27]. These last represent the reinforcing elements (having an axial modulus in the range from 134 to 160 GPa [28]) of the hierarchical structure of plant fibers. Since cellulose is a semi-crystalline polysaccharide, its amorphous fraction can absorb water (due to the high percentage of hydroxyl groups) thus leading to noticeable decrements of the overall tensile stability of the fiber, that became more flexible as a result of plasticization effect [29]. In particular, the rigidity of the cellulose structure is destroyed by the water molecules in the cellulose network structure in which water acts as a plasticizer and it permits cellulose molecules to move freely [30]. Furthermore, the presence of NaCl salt in the solution contributes to the flax fiber degradation. As observed by Yan and Nawawi [31] seawater leads to faster degradation in tensile

strength compared to natural water one. In particular, they observed a reduction of tensile and flexural performances of flax composites up to 20% comparing seawater and water aging. NaCl in the seawater is dissolved as cations and anions that in turns are able to penetrate into the composite structure, thus stimulating local damage within the matrix, fibers and at their interface. Furthermore, the presence of salt ions in the composite interface can improve osmotic diffusion of water at the fiber/matrix interface which accelerate interfacial debonding phenomena [32]. As a consequence, a reduction of the bearing stress at high E/D values occurred, related to the triggering of net tension as main failure mechanism for this specific joint geometry.

Furthermore, the cleavage mechanism should not take place in shear out/bearing failure mechanism transition. However, the mechanical behavior of this geometric configuration observed at high E/D ratios (as shown in Figure 4) is related not to an exclusive bearing failure mechanisms but a mixed bearing/net tension fracture mode was also identified. This implies that the cleavage mode can occur for the intermediate values of E/D also for batch A, where the failure mechanism is mainly dominated by bearing, occasionally with net tension failure mechanisms [16].

3.1.2 Pinned joints with 8 mm hole diameter

Figure 5 shows the evolution of the stress (calculated according to eq. 1) versus displacement curves for samples with 8 mm hole diameter and 12 mm edge distance at varying aging cycles.
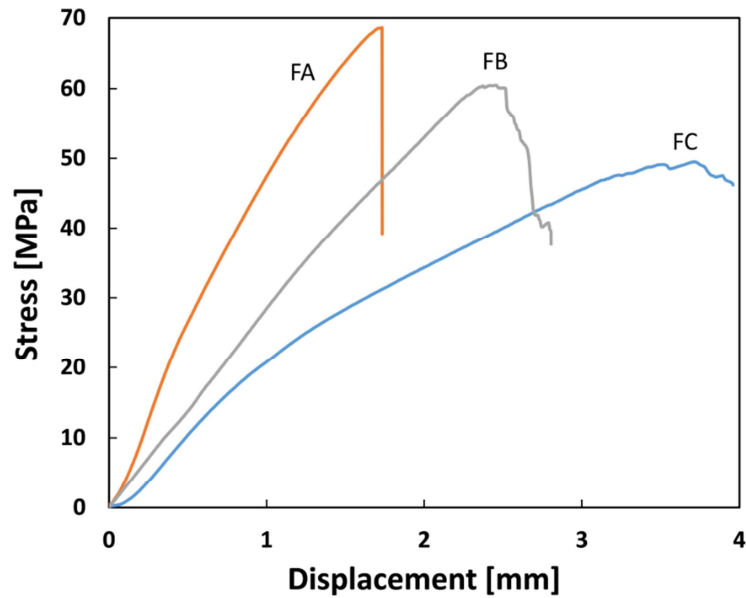
Figure 5. Stress-displacement curves at increasing aging time for pin loaded laminates (D = 8 mm; E = 12 mm; W = 15 mm)

Also in this case a progressive decrease of maximum stress was observed at increasing aging time exposition (i.e., 12% and 27% lower than that of unaged one, for batch B and C, respectively). Similarly, the material suffers a relevant softening effect confirmed by the reduction of stress/displacement coupled to a relevant increase in the displacement at failure. After 60 days of aging (samples FC-8-12-15), flax laminate is characterized by a displacement at failure about three times longer than FA-8-12-15 unaged sample.

Due to their high content in hemicellulose and cellulose and to the presence of voids and cracks within thermoset matrix, flax fibers tend to absorb great amount of water when composites are exposed to aggressive environment such as marine [33] [34]. These results are in accordance with a wide literature that clearly evidence how the mechanical properties of flax fiber composites are greatly influenced by exposition to humid environmental conditions [25] [35].
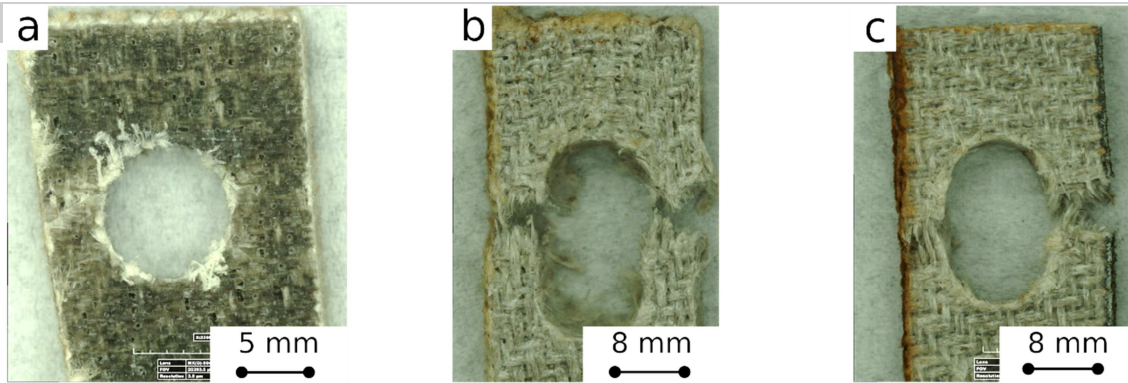
Figure 6. Fracture images of a) FA-8-12-15 b) FB-8-12-15 and c) FC-8-12-15 flax samples

A catastrophic fracture type was observed, as confirmed by the abrupt and sudden drop of the failure stress after reaching the maximum value. This catastrophic and brittle fracture mechanism can be considered typical for brittle thermoset matrices based composites [36]. However, the collapse mechanism of the joint due to the crack triggering in the neighboring area of the hole occurs suddenly for the FA-8-12-15 specimen (i.e., unaged). Instead, on samples with long aging times, the mechanical joint failure occurs prematurely at low stress level but it is characterized by a non-abrupt reduction of the stress: i.e., a slight and gradual decrease of the stress after the reaching of the maximum value can be highlighted. This different behavior, more evident as higher is the aging time, can be ascribed to the matrix plasticization in addition to the chemical and physical degradation phenomena that happens (i.e., penetration with water molecules inside the composite structure of Na^+ cations and Cl^- anions, fiber swelling etc.).

The fracture surfaces of the specimens (Figure 6), visually clarify that all the specimens showed a net tension fracture mechanism. However, the unaged laminates show a neat fracture surface, typical of tensile failures of fiber reinforced thermoset polymers. Vice versa, it was shown for aged specimens (i.e., FB-8-12-15 and FC-8-12-15) both a progressive detachment of the fibers from the matrix and fiber breaking due to the

15

tensile properties of the flax fibers.

Figure 7 shows the maximum stress evolution at increasing edge distance E for pin loaded laminates with hole diameter D = 8 mm and width W = 15 mm, for all aged batches.
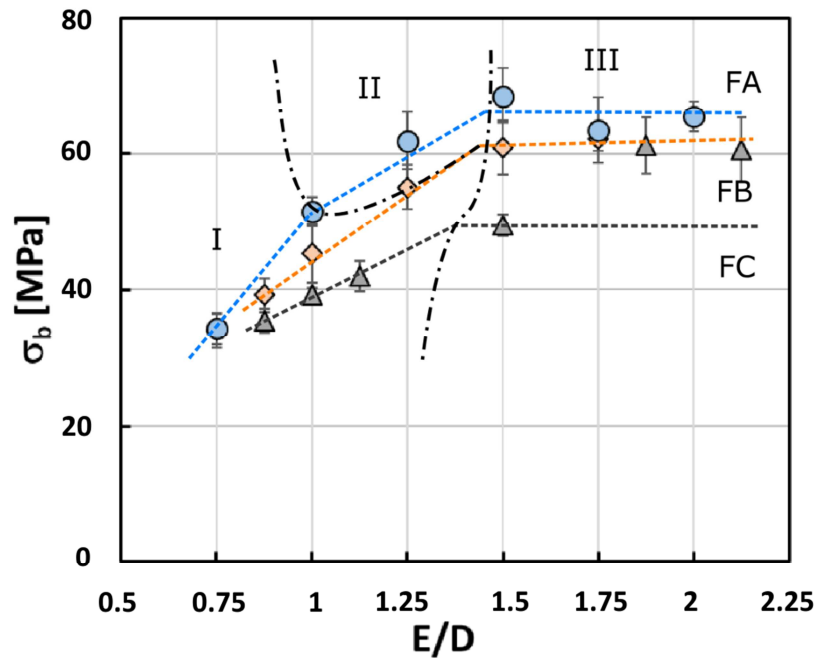

Figure 7. Maximum bearing stress evolution at increasing edge distance E for pin loaded laminates with hole diameter D = 8 mm and width W = 15 mm for all batches

At low edge distance (i.e., E/D <1.0), the mechanical instability of the joint takes place at very low stress level. For this geometry configurations, the shear out is the predominant failure mechanism (region I) due the low distance of the hole from the free edge. The failure stress increases at increasing E/D distance up to edge distance, E, equal to 8 mm. A slight modification of slope trend can be identified for FA batch where for E/D=1 a transition from shear out to cleavage failure mode occurred (region II). This trend is maintained for E/D up to 1.5, where E distance is 12 mm, afterwards the net tension mode happens as failure mechanism and the maximum stress reaches a

batches during the transition from shear out (low E/D values) to net tension (high E/D values) failure mechanism.

Unlike as observed on specimens with a 4 mm hole diameter, the maximum bearing stress at increasing E/D for these samples has similar trend between unaged and 30 days aged samples. Only a slight difference can be highlighted for intermediate E/D values where FA samples showed a more affordable mechanical stability. For this joint configuration, characterized by a high hole diameter, the maximum stress is strongly influenced by catastrophic fracture mechanisms such as shear out and net tension for low and high E values, respectively. Consequently, not showing a bearing failure, the maximum stress reaches lower values than in the previous case (i.e. about 50-60 MPa for 8-12-15 samples with respect to 125-190 MPa for 4-16-15 samples).

Different considerations can be made by analyzing the maximum stress evolution versus E/D ratio of the 30-day samples in a salt spray chamber. Very long aging times have led to a significant reduction of the maximum stress, especially for intermediate values of the E/D ratio. There is no observed a clear cleavage region and a more abrupt transition from shear out to net tension occurred.

In this case, the great amount of water absorbed by flax laminates (~12% [33]) weakens fiber-matrix adhesion, leading to decrease the shear resistance of the specimens. This justifies the high reduction of failure stress at intermediate and high E/D values due to a premature fracture for shear out or net tension mechanism experienced by flax composite laminates. Furthermore, it can be considered the formation of preferential pathways for the water diffusion toward the flax fibers due to hydrophilic nature of their components. Cause of water molecules interaction, a further degradation at the fiber-matrix interface can be stimulated by local removal of hydrophobic structural natural fiber components, such as hydrocarbons, waxes, and/or lignin [37]. This phenomenon is

Furthermore, it is speed up due to the presence of preferential pathways (voids, cracks) in the matrix bulk due to aging environmental exposure or to the manufacturing process [39].

Consequently, the shear out mechanism becomes the predominant ones for a wider range of geometrical conditions, so hiding the net tension contribution. This last mechanism goes back to be predominant just for higher value of E/D ratio.

3.2 Evolution of failure mechanisms at varying joint geometry

The previous considerations have been summarized in Figure 8 where topological graphs of the failure mechanisms that take place at varying the joint geometric parameters have been reported.
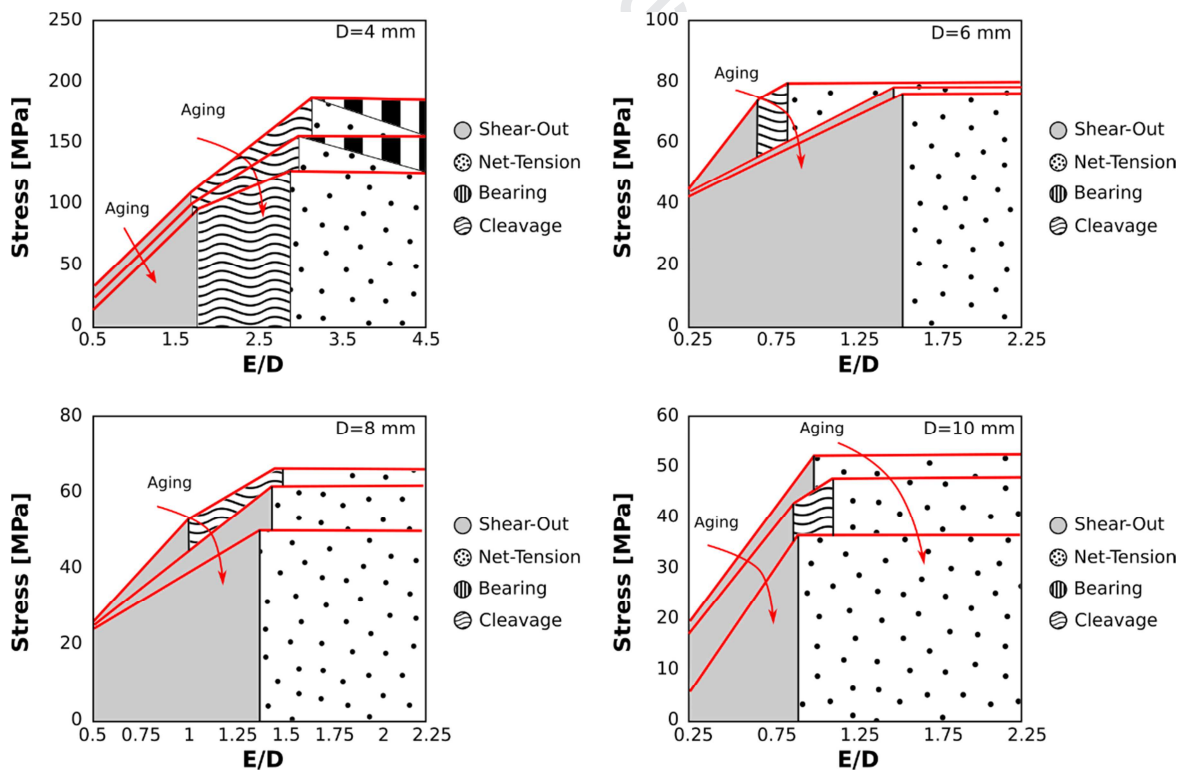
Figure 8. Scheme of failure mechanisms evolution in bearing stress vs E/D plot for all laminates

Depending on hole diameters some damage phenomena can be identified:

18

- Small hole diameter (i.e., D = 4 mm): the fracture evolves from shear out to bearing/net tension, at increasing E/D ratio. A large region where occurred cleavage or mixed net-tension/shear out fracture is detected for intermediate E/D ratios (i.e., range about 1.75-3.0). The environmental aging also induces a noticeable reduction of the failure stress for samples with high E/D values.

- Medium hole diameter (i.e., D = 6-8 mm): The graphs related to joint geometry with larger hole diameters differ significantly from the previous one. In particular, there are no evident cleavage areas, especially for aged specimens. This behavior can be related to the lower tensile and shear resistance of the aged flax laminate. FB and FC batches, compared to FA one, have a wider joint geometric configuration where the shear out fracture occurred. In particular, for medium E values, for all batches, a premature fracture for shear out can be highlighted for hole diameter D=6 and D=8. This behavior may be attributed to the specific joint geometry where the difference between hole diameter and sample width is still relevant thus limiting net tension fracture mechanism only at high E/D values. This extensive area in shear out failure mechanism is also favored by the reduced interfacial adhesion at the fiber/matrix interface that activate shear cracks propagation in the pin/hole contact area, preventing a mixed failure mechanism for cleavage.

- Large hole diameter (i.e., D = 10 mm): In this case, net tension becomes the dominant fracture mechanism for large E values (large E/D ratio). All batches show quite similar fracture modes ranges. However, significant differences can be found in the mechanical performance of the joint. There is a significant reduction in the maximum stress at high E/D joint geometries. In particular, FB and FC samples, for E/D>1.25, showed a maximum stress about 12% and 31% lower than unaged sample, respectively. As already stated, this trend has been attributed to the reduced tensile strength induced by the aging effect (matrix and fiber softening coupled with
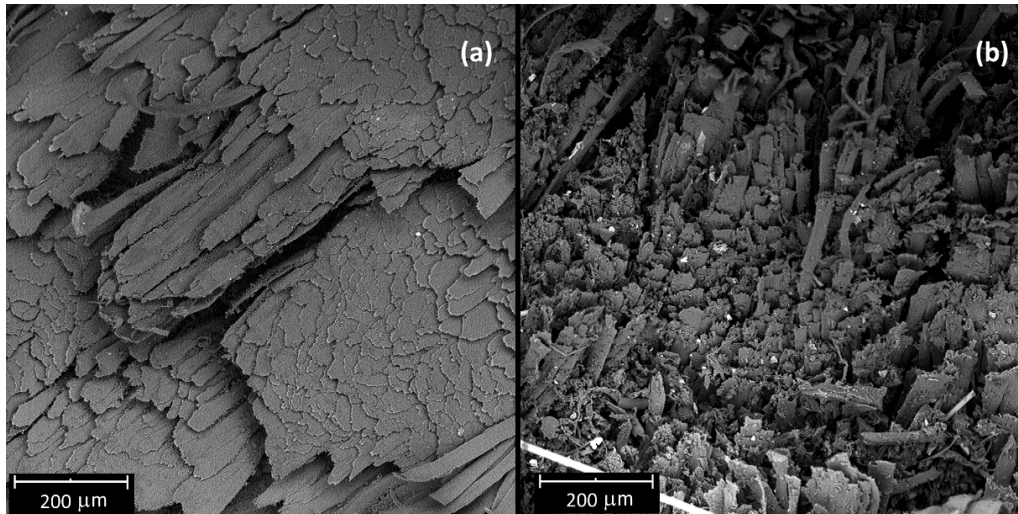
interface).

Figure 9. SEM images of a) un-aged b) and 60 days aged flax composite laminates

SEM images of the cross-section of unaged and 60 days aged composites (i.e. FA and FC) are shown in Figure 9. Unaged sample is characterized by structure with not relevant voids or heterogeneities (Figure 9a). Nevertheless, debonding phenomena at the fiber-matrix interface can be highlighted, due to the low compatibility between hydrophilic flax fibers and hydrophobic epoxy matrix. This leads to the formation of bundle clusters with a good interaction but almost completely detached from the neighboring area. This morphology is prone to activate detrimental degradation phenomena when the composite structure operates in severe environmental conditions. This is confirmed by analyzing Figure 9b (i.e., cross section of 60 days aged sample) in which very extended damaged area are visible due to an evident interfacial debonding. This phenomenon is largely diffused on the whole cross section and no bundle clusters with compact structure are observable. The damaged area is probably responsible for the triggering and propagation of cracks that significantly reduces the mechanical performances of the flax laminate after long aging time.

Further information about the mechanical performances reduction of composite joint induced by aging exposition can be acquired analyzing the strength limits variation at increasing aging days in salt-fog chamber. Figure 10 shows the evolution of strength failure limits for the three main fracture mechanisms (i.e. bearing, net tension and shear out) observed for all laminate batches.
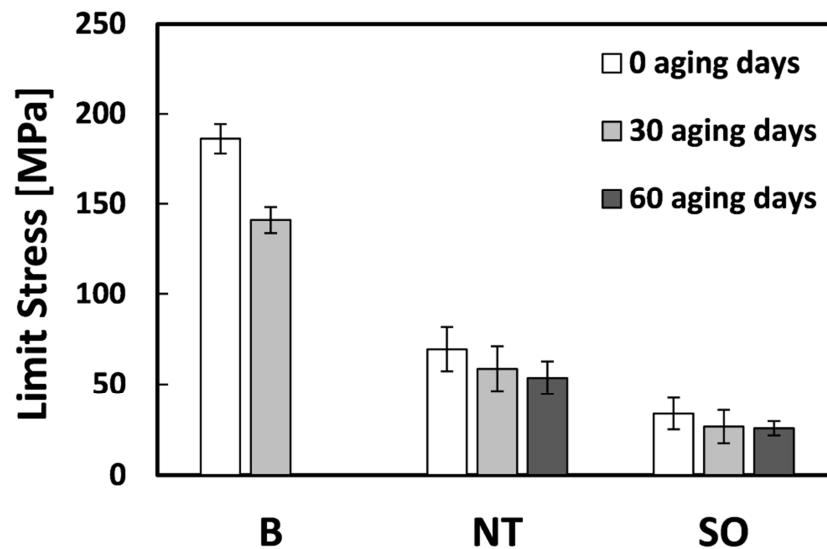

Figure 10. Bearing (B), Net tension (NT) and Shear out (SO) stress limits experimentally determined for all composite laminates

A clear dependence of bearing resistance from aging time can be highlighted. The bearing limit stress, just after 30 days of aging in the salt spray chamber, undergoes a reduction of about 18% compared to the unaged laminate. For batch C, characterized by 60 days of aging, no bearing failure happened for any sample configuration so that bearing limit stress was not acquired.

On the contrary, a less abrupt degradation effect can be observed by analyzing the variation of NT and SO stress limits. For both failure conditions there is a slight progressive reduction of the limit stresses with increasing aging time, with a reduction of 23-24% after 60 days of aging (21% and 23% after 30 aging days for NT and SO limit stress, respectively). These results are summarized in Table 1.

21

Table 1. Bearing (B), Net tension (NT) and Shear out (SO) stress limits and their percentages of reduction at varying aging time compared to FA batch

Aging time [days]	Limit Stress [MPa]			Reduction [%]		
	B	NT	SO	B	NT	SO
0	191	69.4	33.6	--	--	--
30	156	55.1	25.9	18 %	21 %	23 %
60	NO	53.5	25.5		23 %	24 %

3.4   Pinned joint failure maps

In order to better discriminate how the joint geometry influences its failure mechanism, a topological failure map of the FB flax laminates (i.e. 30 days aged laminates) at varying E/D and W/D ratios (X and Y axis, respectively) is shown in Figure 11. The types of fracture, experimentally observed for each combination of joint geometric parameters, has been highlighted by associating each failure mechanism with a marker color in order to better highlight the representative clusters of a specific form of damage.
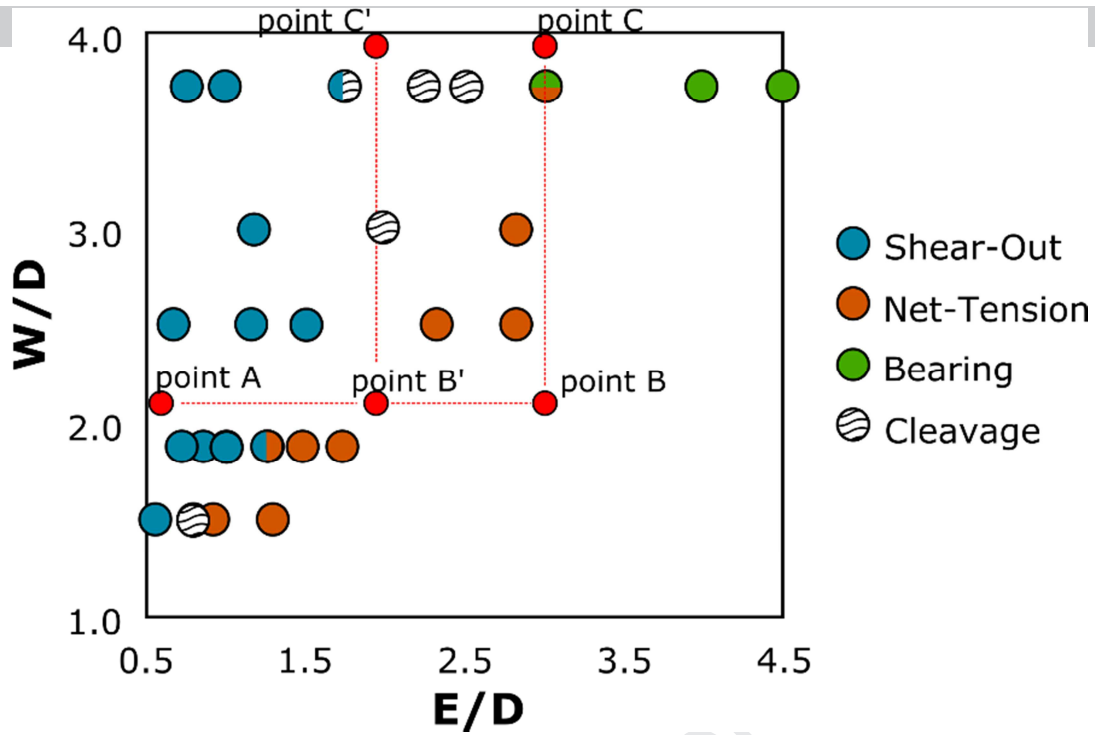
Figure 11. Failure mechanisms in E/D versus W/D plot for FB batch

Four well-defined clusters, each one related to a definite failure mechanism, can be identified:

I. The bearing fracture, green circle marker, is located in a narrow area in the right-high corner of the map, indicating that it becomes the main failure mechanism for joint geometries characterized by W/D and E/D values higher than 2.5 and 3.75, respectively;

II. Net tension is the pre-dominant failure mechanism for high E/D and medium and low W/D ratios. This behavior is related to large hole diameters (i.e., low W/D ratio) and high edge distances (i.e., high E/D ratio). For these geometrical configurations the pinned composite is constituted by a small cross-section area, orthogonal to applied load. This implies that a high stress level can be reached in this cross-section, thus triggering a premature and catastrophic net tension fracture, due to the activation and propagation of tensile cracks in the composite laminate;

III. Conversely, the cluster related to shear out failure mode can be identified for low E/D and high W/D ratios. This joint configuration is characterized by a very low E distance. The joint hole is located close to the free sample edge, involving a limited cross section area just behind the pin/hole contact area, able to suffer shear stress. Therefore, a premature shear out is the pre-dominant premature failure mechanism for this geometrical configuration;

IV. Moreover, a further cluster due to cleavage failure mechanism can be highlighted, identified as a transition cluster between net tension and shear out ones. It is a catastrophic joint failure occurring with an extended damaged zone in the peripheral hole area, due both to mixed net tension and shear out crack propagation [40] [41]. However, this region becomes gradually less representative at increasing both of E/D and W/D ratios. This may be associated with the greater joint instability for these geometric configurations which implies a higher sensitivity to fractures at low stress for the failure mechanism that first takes place [42].

Since a progressive damage mechanism allows to identify the occurring damage risk, acting as a warning and contributing significantly to the safety of the structural components, the bearing failure of the joints represents the recommended and preferred joining design solution. Vice versa, net tension, shear out and cleavage failure take place with an abrupt fracture of the structure not allowing to provide a warning of the occurring damage risk. Consequently, these catastrophic failures must be avoided. Based on the failure mechanisms clusters in the map (Figure 11), a sufficiently high W/D ratio in the composite joints is required at the design stage to exclude failure by net tension. Similarly, high E/D ratios preclude the risk of a shear out failure. The combination of the above conditions is the expected design choice, representing the joint configuration suitable to achieve a gradual bearing fracture. However, the excess

of material required to guarantee the stability of the joint represents a limit for the effective development of composite materials as a structural element. Therefore, it is absolutely necessary to provide forecasting damage procedures able to predict the damage at varying joint geometry. The proposed failure map approach represents an effective and suitable precondition for a correct design of the pinned composite joints, considering the simplicity and adaptability to the environmental aging conditions in which the structure operates.

By analyzing in more detail Figure 11 it is possible to observe that, for low values of W/D and E/D (point A), the dominant failure mechanism is shear out. Starting from this point, by increasing E/D and keeping constant W/D, a transition between shear out and net tension takes place (point B and point B') through an intermediate fracture condition by cleavage. This behavior is justified since, by increasing the hole distance from the free edge E, there is a significant increase of the resistant area located just behind the hole responsible for the shear out collapse of the joint. At the same time, the relatively high diameter of the hole (i.e., low W/D) indicates that the transversal cross section of the laminate is small enough to favor the net tension fracture. Afterward, depending on E/D value, a subsequent increase of W/D ratio, maintaining constant E/D parameter can induce a different mechanical behavior of the pinned laminate. In particular, for high E/D values (point B) a transition to bearing can be observed by increasing W/D. The reduction of hole diameter (i.e., W/D increases) significantly increases the net tension failure load stimulating the preferred progressive bearing fracture (point C). However, a reverse transition toward shear out can be highlighted for intermediate E/D values (point B'). For this joint configuration, although large W/D are considered the E parameter is too small stimulating a premature fracture by shear-out (point C').

Based on the geometrical characteristics of the joint it is possible to theoretically forecast the occurring fracture mechanism by using the relationship between bearing,

25

the fracture transition lines in the E/D–W/D plane, can be defined in order to divide the

failure plane into three zones, discriminating the fracture mechanisms regions located in

fracture plots, as reported in Figure 11. By equalizing the threshold failure loads for

each fracture mechanism, calculated on the basis of the experimental values of stress

limits for bearing, net tension and shear out, it is possible to represent the following

equations (Eq.2, Eq.3 and Eq.4), which can be associated to the transitions among the

different fracture mechanisms:

Bearing/Net tension
$$\frac{W}{D} = \sigma_B/\sigma_{NT} + 1$$
Eq. 2

Bearing/Shear out
$$\frac{E}{D} = 1/2 \cdot \sigma_B/\tau_{SO}$$
Eq. 3

Shear out/Net tension
$$\frac{W}{D} = 2 \cdot \sigma_{SO}/\sigma_{NT} \cdot e/d + 1$$
Eq. 4

σ_B, σ_{NT} and τ_{SO} are the bearing, net tension and shear out strengths, respectively. The

above strengths can be calculated with the following equations (Eq.5, Eq.6 and Eq.7):

$$\boldsymbol{\sigma_B} = \frac{P_{max}}{D \cdot t}$$
Eq. 5

$$\sigma_{NT} = \frac{P_{max}}{(W-D) \cdot t}$$
Eq. 6

$$\tau_{SO} = \frac{P_{max}}{2 \cdot E \cdot t}$$
Eq. 7

Where P_{max} is the maximum load. D, W, t and E are the hole diameter, width and

thickness of the sample and the hole center distance from the sample free edge,

respectively.

Based on equations 2-4 a failure map can be defined [17], a theoretical forecasting

approach can be applied on data in Figure 11 to predict transition transient areas. In

Figure 12a, the good match between theoretical and experimental results is evidenced

proving a good reliability for the flax composite laminates.

In particular, on the basis of the topological fracture map shown in Figure 12a, it is noted that, for a 30 days aged flax laminate, it is necessary to set geometric ratios E/D and W/D higher than 2.5 and 3.3, respectively. For these geometric joint configurations, the fracture mechanism that can be found is bearing, the preferred one due to its progressive and non-catastrophic nature.

As discussed above, net tension and shear out are instead premature fracture mechanisms that are not desirable in design due to their catastrophic nature. This implies that, as soon as the triggering of local damage occurs, a sharp reduction in joint resistance and a subsequent collapse in performances takes place. This behavior was not verified for the pinned joints which fail through bearing failure mode, which showed a high maximum resistance and displacement before fracture, indicating the progressive and not catastrophic nature of this type of failure mode.

Several failure mechanisms play an important role in the initiation of bearing damage of pinned laminates [44], such as micromechanical fiber buckling in the laminate [45] or delamination damage [46], thus favoring a progressive fracture that prevents unwanted faults.

Another relevant issue that makes the bearing fracture suitable for the joining design in composite material, compared to the other competing failure modes, is that, after the beginning of the bearing damage, the joints still have a good residual strength and an adequate mechanical stability. This is a fundamental precondition under operating conditions, allowing identification of warning conditions during inspection and maintenance operations if necessary. It preserves the structural composite component from an accidental and unexpected mechanical fault.

The knowledge on damage modes triggering and propagation and how they evolve due to an environmental degradation of the structure, is an aspect to be taken into account and particularly felt in research and applied design. In such a context, Figure 12b shows

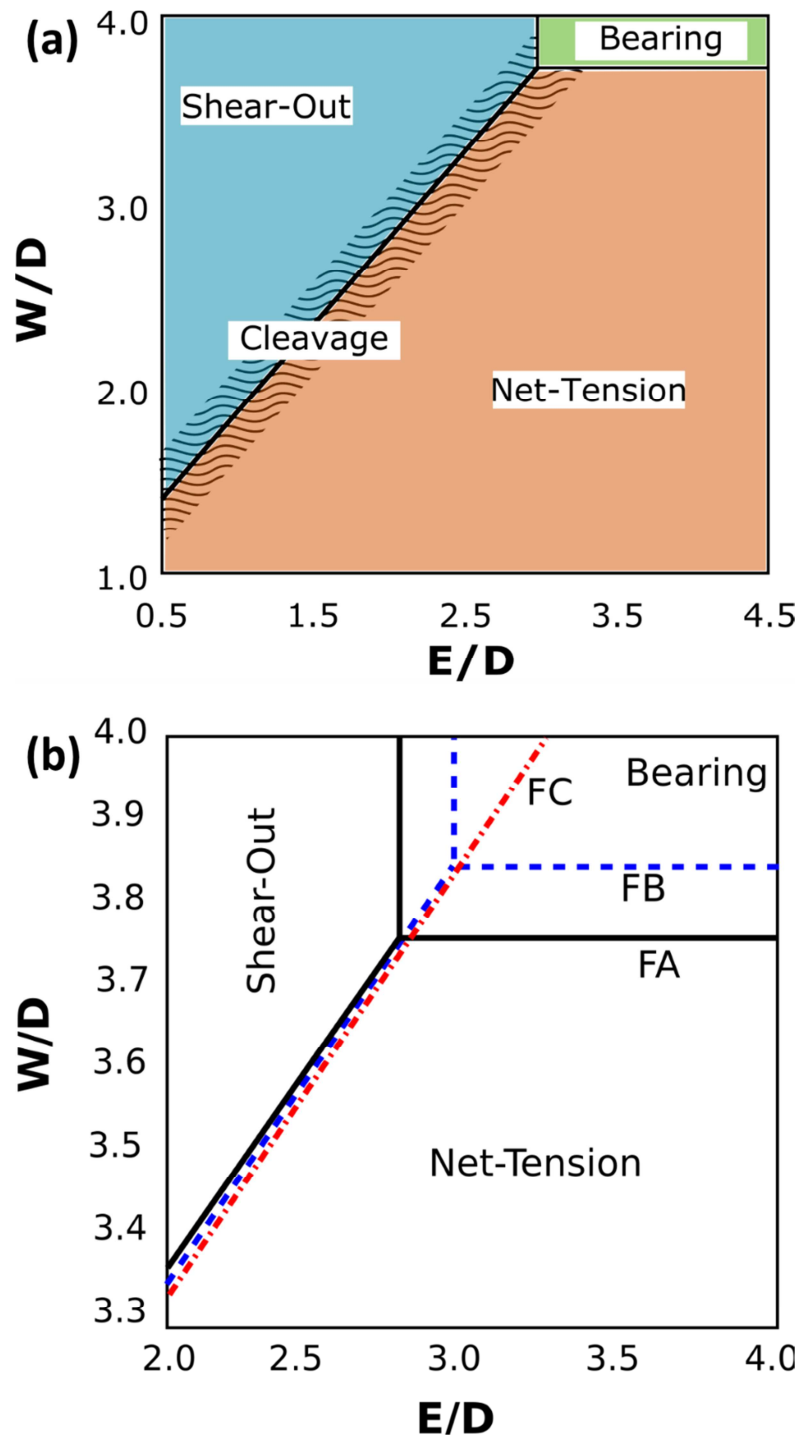time in a salt spray chamber.

Figure 12. Failure map in E/D versus W/D plot for (a) FB batch and (b) at increasing aging time

The degradation of the composite laminate, imposed by the critical environmental conditions to which it was subjected, led to a progressive reduction of the bearing region, located in the upper right corner of the map. In particular, for 60 days aged specimens, the bearing region is not identified in the chosen E/D and W/D ratios.

After only 30 days of aging, the W/D threshold that defines the transition between net tension and shear out is quite constant (i.e. from 3.75 to 3.83)

Instead, a slight increase in the E/D ratio, which defines the transition between net tension and bearing, of about 6% (i.e., from 2.84 to 3.01) can also be observed after 30 days of aging. There are no significant differences in the transition between net-tension and shear out.
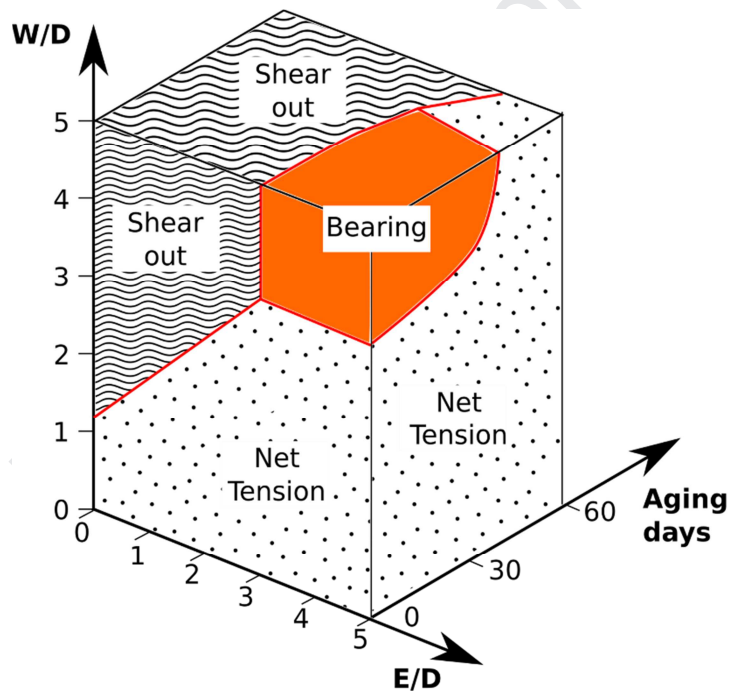
Figure 13. 3D failure mechanisms map in E/D versus W/D plot at varying aging time

In order to improve the fracture map readability of the aging time effect and to allow a better discrimination of the fracture modification at varying the joint geometry, a 3D representation of the fracture map has been also proposed. By analyzing Figure 13, it can be seen that the bearing region is identifiable only for low aging times. On the other hand, the net tension and shear out regions become more and more extended with

29

clearly related to the particular sensitivity of natural flax fibers to this aggressive environment. The natural fibers undergo significant degradation which reduces adhesion at the fiber/matrix interface, but mainly reduces the tensile strength of the fiber itself. This entails an exaltation of the catastrophic premature fracture for net tension and shear out.

A further relevant outcome of this paper was to highlight that the environmental aging of full flax laminates induces a reduction of the bearing area in the failure map thus limiting the effective mechanical durability of the mechanical joint. Therefore, in order to achieve and design structural joints that fails by bearing mode, thus avoiding catastrophic failures, pinned composite laminates need be designed by selecting specific geometrical parameters (i.e., E/D and W/D ratios) in a narrow range of values in order to guarantee a joint stability also at long aging time. The purpose is to minimize the failure issue related to premature fracture due to shear out and net tension, thus improving the mechanical stability of pin-loaded laminates.

The durability of flax laminates is strongly affected by environmental conditions, so these experimental results and the proposed predictive topological maps, represent a promising approach aimed to define effective and suitable design methods that integrate the conventional knowledge on mechanical stability of the joint with the evolution of the structure performance in real working environmental conditions of the composite structure.

Conclusions

The present paper deals with the evaluation of the effect of salt-fog exposition on the bearing behavior of pinned flax/epoxy composites. To this scope, drilled samples at varying geometrical configuration (i.e., hole diameter (D), edge distance (E) and sample width (W)) were exposed to salt-fog spray up to 60 days, according to ASTM B 117 standard.

The experimental results showed that salt-fog exposition noticeably alters the mechanical performances of the pinned flax/epoxy composite. Due to this, a progressive modification of damage mechanism transitions occurred in the failure map at increasing the aging exposition time. In particular, salt-fog induces a reduction of the bearing area in the failure map thus favoring premature and catastrophic shear out and net tension failure mechanisms and, as a consequence, limiting the effective mechanical durability of the mechanical joint.

Overall, from the achieved experimental results it is possible to state that:

− In order to avoid catastrophic failures of structural joints and favor only a progressive failure mode (i.e., bearing), pinned flax/epoxy laminates need be designed by selecting specific geometrical parameters (i.e., E/D and W/D ratios) in a narrow range of values in order to guarantee a joint stability also after long exposition to salt-fog conditions;

− Due to the great influence of environmental conditions on the durability of flax laminates, the experimental results and the proposed predictive topological maps can be considered as a promising tool to integrate the conventional knowledge on the mechanical joint stability.

References

[1]   Shivakumar KN. Carbon/Vinyl Ester Composites for Enhanced Performance in Marine Applications. J Reinf Plast Compos 2006;25:1101–16. doi:10.1177/0731684406065194.

[2]   Cao J, Grenestedt JL. Design and testing of joints for composite sandwich/steel hybrid ship hulls. Compos Part A Appl Sci Manuf 2004;35:1091–105. doi:10.1016/j.compositesa.2004.02.010.

[3]   Caccese V, Kabche J-P, Berube KA, Boone MJ. Structural response of a hybrid composite/aluminum strut assembly. Compos Struct 2007;80:159–71. doi:10.1016/j.compstruct.2006.04.075.

[4]   Valenza A, Fiore V, Fratini L. Mechanical behaviour and failure modes of metal to composite adhesive joints for nautical applications. Int J Adv Manuf Technol 2011;53:593–600.

[5]   Valenza A, Fiore V, Borsellino C, Calabrese L, Di Bella G. Failure Map of Composite Laminate Mechanical Joint. J Compos Mater 2007;41:951–64. doi:10.1177/0021998306067257.

[6]   Calabrese L, Fiore V, Scalici T, Bruzzaniti P, Valenza A. Failure maps to assess bearing performances of glass composite laminates. Polym Compos 2018. doi:10.1002/pc.24806.

[7]   Ozen M, Sayman O. Failure loads of mechanical fastened pinned and bolted composite joints with two serial holes. Compos Part B Eng 2011;42:264–74. doi:10.1016/j.compositesb.2010.10.003.

[8]   Feo L, Marra G, Mosallam AS. Stress analysis of multi-bolted joints for FRP pultruded composite structures. Compos Struct 2012;94:3769–80. doi:10.1016/j.compstruct.2012.06.017.

[9] Singh M, Saini JS, Bhunia H. To study the contribution of different geometric parameters on the failure load for multi holes pin joints prepared from glass/epoxy nanoclay laminates. J Compos Mater 2018;52:629–44. doi:10.1177/0021998317712572.

[10] Okutan B, Aslan Z, Karakuzu R. A study of the effects of various geometric parameters on the failure strength of pin-loaded woven-glass-fiber reinforced epoxy laminate. Compos Sci Technol 2001;61:1491–7. doi:10.1016/S0266-3538(01)00043-4.

[11] Vangrimde B, Boukhili R. Bearing stiffness of glass fibre-reinforced polyester: Influence of coupon geometry and laminate properties. Compos Struct 2002;58:57–73. doi:10.1016/S0263-8223(02)00039-9.

[12] Abdullah MS, Abdullah AB, Hassan MH, Samad Z. Bearing strength and progressive failure analysis of the punched hole of CFRP under tensile loading. Int J Adv Manuf Technol 2018;97:1–9. doi:10.1007/s00170-018-2091-x.

[13] Yilmaz T, Sinmazcelik T. Bearing strength of Pin-Connected polymer composites subjected to dynamic loading. Polym Compos 2010;31:25–31. doi:10.1002/pc.20843.

[14] Turan K, Gur M, Kaman MO. Progressive failure analysis of pin-loaded unidirectional carbon-epoxy laminated composites. Mech Adv Mater Struct 2014;21:98–106. doi:10.1080/15376494.2012.677109.

[15] Yýlmaz T, Sýnmazçelik T. Investigation of load bearing performances of pin connected carbon/polyphenylene sulphide composites under static loading conditions. Mater Des 2007;28:520–7. doi:10.1016/j.matdes.2005.08.015.

[16] Fiore V, Calabrese L, Scalici T, Bruzzaniti P, Valenza A. Experimental design of the bearing performances of flax fiber reinforced epoxy composites by a failure map. Compos Part B Eng 2018;148:40–8.

[17] Fiore V, Calabrese L, Scalici T, Bruzzaniti P, Valenza A. Bearing strength and failure behavior of pinned hybrid glass-flax composite laminates. Polym Test 2018;69:310–9. doi:10.1016/j.polymertesting.2018.04.041.

[18] Quinn WJ, Matthews FL. The Effect of Stacking Sequence on the Pin-Bearing Strength in Glass Fibre Reinforced Plastic. J Compos Mater 1977;11:139–45. doi:10.1177/002199837701100202.

[19] Sola C, Castanié B, Michel L, Lachaud F, Delabie A, Mermoz E. On the role of kinking in the bearing failure of composite laminates. Compos Struct 2016;141:184–93. doi:10.1016/j.compstruct.2016.01.058.

[20] Fiore V, Scalici T, Calabrese L, Valenza A, Proverbio E. Effect of external basalt layers on durability behaviour of flax reinforced composites. Compos Part B Eng 2016;84:258–65. doi:10.1016/j.compositesb.2015.08.087.

[21] Opelt C V., Cândido GM, Rezende MC. Compressive failure of fiber reinforced polymer composites – A fractographic study of the compression failure modes. Mater Today Commun 2018;15:218–27. doi:10.1016/j.mtcomm.2018.03.012.

[22] Malmstein M, Chambers AR, Blake JIR. Hygrothermal ageing of plant oil based marine composites. Compos Struct 2013;101:138–43. doi:10.1016/j.compstruct.2013.02.003.

[23] Abd-El-Naby SFM, Hollaway L. The experimental behaviour of bolted joints in pultruded glass/ polyester material. Part 1: Single-bolt joints. Composites 1993;24:531–8. doi:10.1016/0010-4361(93)90266-B.

[24] Turvey G. Failure of single-lap single-bolt tension joints in pultruded glass fibre reinforced plate. 6th Int. Conf. Compos. Constr. Eng., Rome (Italy): 2012.

[25] Assarar M, Scida D, El Mahi A, Poilâne C, Ayad R. Influence of water ageing on mechanical properties and damage events of two reinforced composite materials:

35

Flax-fibres and glass-fibres. Mater Des 2011;32:788–95. doi:10.1016/j.matdes.2010.07.024.

[26] Baley C, Le Duigou A, Bourmaud A, Davies P. Influence of drying on the mechanical behaviour of flax fibres and their unidirectional composites. Compos Part A Appl Sci Manuf 2012;43:1226–33. doi:10.1016/j.compositesa.2012.03.005.

[27] Bos HL, Van Den Oever MJA, Peters OCJJ. Tensile and compressive properties of flax fibres for natural fibre reinforced composites. J Mater Sci 2002;37:1683–92. doi:10.1023/A:1014925621252.

[28] Mohanty AK, Misra M, Hinrichsen G. Biofibres, biodegradable polymers and biocomposites: An overview. Macromol Mater Eng 2000;276–277:1–24. doi:10.1002/(SICI)1439-2054(20000301)276:1<1::AID-MAME1>3.0.CO;2-W.

[29] Akil HM, Cheng LW, Mohd Ishak ZA, Abu Bakar A, Abd Rahman MA. Water absorption study on pultruded jute fibre reinforced unsaturated polyester composites. Compos Sci Technol 2009;69:1942–8. doi:10.1016/j.compscitech.2009.04.014.

[30] Dhakal HN, Zhang ZY, Richardson MOW. Effect of water absorption on the mechanical properties of hemp fibre reinforced unsaturated polyester composites. Compos Sci Technol 2007;67:1674–83. doi:10.1016/j.compscitech.2006.06.019.

[31] Yan L, Chouw N. Effect of water, seawater and alkaline solution ageing on mechanical properties of flax fabric/epoxy composites used for civil engineering applications. Constr Build Mater 2015;99:118–27. doi:10.1016/j.conbuildmat.2015.09.025.

[32] Ashbee KHG, Wyatt RC. Water damage in glass fibre/resin composites. Proceeding R Soc A 1969;53:312–553. doi:10.1098/rspa.1969.0175.

[33] Calabrese L, Fiore V, Scalici T, Valenza A. Experimental assessment of the

improved properties during aging of flax/glass hybrid composite laminates for marine applications. J Appl Polym Sci 2019;136:47203. doi:10.1002/app.47203.

[34] Le Duigou A, Davies P, Baley C. Seawater ageing of flax/poly(lactic acid) biocomposites. Polym Degrad Stab 2009;94:1151–62. doi:10.1016/j.polymdegradstab.2009.03.025.

[35] Scida D, Assarar M, Poilâne C, Ayad R. Influence of hygrothermal ageing on the damage mechanisms of flax-fibre reinforced epoxy composite. Compos Part B Eng 2013;48:51–8. doi:10.1016/j.compositesb.2012.12.010.

[36] Ouarhim W, Zari N, Bouhfid R, Qaiss A el kacem. Mechanical performance of natural fibers–based thermosetting composites. Mech. Phys. Test. Biocomposites, Fibre-Reinforced Compos. Hybrid Compos., 2019, p. 43–60. doi:10.1016/B978-0-08-102292-4.00003-5.

[37] Peng Y, Liu R, Cao J, Chen Y. Effects of UV weathering on surface properties of polypropylene composites reinforced with wood flour, lignin, and cellulose. Appl Surf Sci 2014;317:385–92. doi:10.1016/j.apsusc.2014.08.140.

[38] Sahoo SK, Mohanty S, Nayak SK. Mechanical, Thermal, and Interfacial Characterization of Randomly Oriented Short Sisal Fibers Reinforced Epoxy Composite Modified with Epoxidized Soybean Oil. J Nat Fibers 2017;14:357–67. doi:10.1080/15440478.2016.1212757.

[39] Fiore V, Scalici T, Badagliacco D, Enea D, Alaimo G, Valenza A. Aging resistance of bio-epoxy jute-basalt hybrid composites as novel multilayer structures for cladding. Compos Struct 2017;160:1319–28. doi:10.1016/j.compstruct.2016.11.025.

[40] Fiore V, Calabrese L, Proverbio E, Passari R, Valenza A. Salt spray fog ageing of hybrid composite/metal rivet joints for automotive applications. Compos Part B Eng 2017;108:65–74. doi:10.1016/j.compositesb.2016.09.096.

[41]   Awadhani L V., Bewoor AK. Analytical and experimental investigation of Effect of geometric parameters on the failure modes in a single lap single bolted metal to GFRP composite bolted joints subjected to axial tensile loading. Mater. Today Proc., 2017. doi:10.1016/j.matpr.2017.07.063.

[42]   Ahmad H, Crocombe AD, Smith PA. Strength prediction in CFRP woven laminate bolted single-lap joints under quasi-static loading using XFEM. Compos Part A Appl Sci Manuf 2014. doi:10.1016/j.compositesa.2014.07.013.

[43]   Fiore V, Calabrese L, Scalici T, Bruzzaniti P, Valenza A. Experimental design of the bearing performances of flax fibre reinforced epoxy composites by a failure map. Compos Part B Eng n.d.

[44]   Xiao Y, Ishikawa T. Bearing strength and failure behavior of bolted composite joints (part I: Experimental investigation). Compos Sci Technol 2005;65:1022–31. doi:10.1016/j.compscitech.2005.02.011.

[45]   Wu PS, Sun CT. Bearing failure in pin contact of composite laminates. AIAA J 1998;36:2124–9. doi:10.2514/2.316.

[46]   Camanho PP, Bowron S, Matthews FL. Failure Mechanisms in Bolted CFRP. J Reinf Plast Compos 1998;17:205–33. doi:10.1177/073168449801700302.

Figure 1. (a) Geometry of bearing specimens and (b) schematization of bearing test set-up

Figure 2. Stress-displacement curves at increasing aging time for pin loaded laminates (D = 4 mm; E = 16 mm; W = 15 mm).

Figure 3. Fracture images of a) FA-4-16-15 b) FB-4-16-15 and c) FC-4-16-15 samples.

Figure 4. Maximum bearing stress evolution at increasing edge distance E for pin loaded laminates with hole diameter D = 4 mm and width W = 15 mm (W/D = 3.75) for all batches.

Figure 5. Stress-displacement curves at increasing aging time for pin loaded laminates (D = 8 mm; E = 12 mm; W = 15 mm)

Figure 6. Fracture images of a) FA-8-12-15 b) FB-8-12-15 and c) FC-8-12-15 flax samples.

Figure 7. Maximum bearing stress evolution at increasing edge distance E for pin loaded laminates with hole diameter D = 8 mm and width W = 15 mm for all batches.

Figure 8. Scheme of failure mechanisms evolution in bearing stress vs E/D plot for all laminates.

Figure 9. SEM images of a) un-aged b) and 60 days aged flax composite laminates.

Figure 10.   Bearing (B), Net tension (NT) and Shear out (SO) stress limits experimentally determined for all composite laminates.

Figure 11. Failure mechanisms in E/D versus W/D plot for FB batch.

Figure 12. Failure map in E/D versus W/D plot for (a) FB batch and (b) at increasing aging time

Table Captions

Table 1. Bearing (B), Net tension (NT) and Shear out (SO) stress limits and their percentages of reduction at varying aging time compared to FA batch

- Bearing behavior of pin-loaded flax laminates was investigated in severe environmental conditions;
- The bearing stress evolution and failure mechanisms were evaluated at varying pin diameter and hole to sample free edge distance;
- The salt fog aging induced modification on the mechanical performances of the pinned composite joint;
- Failure map was developed evidencing a progressive modification of damage mechanisms transitions, at increasing aging time;
- Threshold values of E/D and W/D at varying salt-fog exposition time were defined;

Manuscript title: **Evolution of the bearing failure map of pinned flax composite laminates aged in marine environment**

Authors: **Vincenzo Fiore, Luigi Calabrese, Tommaso Scalici, Antonino Valenza**

The authors declare that they have no known competing financial interests or personal relationships that could have appeared to influence the work reported in this paper.

Vincenzo Fiore: Methodology, Data curation, Writing- Original draft preparation, Reviewing and Editing. **Luigi Calabrese:** Conceptualization, Methodology, Investigation, Data curation, Reviewing and Editing. **Tommaso Scalici:** Data curation, Writing- Original draft preparation. **Antonino Valenza**: Supervision.